

FEDSM-ICNMM2010-30932

PREDICTION OF HYDRODYNAMIC NOISE SCATTERED BY THE NON-COMPACT CIRCULAR CYLINDER

Yijun Mao

Datong Qi

Yuanyuan Gu

dtqi@mail.xjtu.edu.cn

School of Energy and Power Engineering, Xi'an Jiaotong University, Xi'an, P.R.China

ABSTRACT

A numerical investigation is carried out to predict the noise radiated from high Reynolds number incompressible flow over the circular cylinder. The study focuses on the scattering effect of cylinder surface to the propagation of noise at different frequencies. A boundary integral equation which extends the acoustic analogy to predict the hydrodynamic noise scattered by the non-compact surface is employed. Methods of unsteady flow simulation and noise prediction are validated by the experimental data and analytical result, respectively. Computational results of the noise at different frequencies show that the diffraction of cylinder surface to low-frequency noise is equivalent to a compact dipole source, but the scattering effect to the high-frequency noise gives a trefoil-like pattern which is much different from the directivity pattern of both quadrupole and dipole sources. Moreover, the advantage of the method is to avoid the time-consuming volume integral, which has to be implemented by using theory of vortex sound and method of the tailored Green's function.

INTRODUCTION

Prediction of the noise radiated from the high Reynolds number and low Mach number turbulent flow over the circular cylinder is an important research topic for its various engineering applications. All prediction methods could be divided into two categories, the first is the direct numerical simulation (DNS) in which the compressible flow field and acoustic field are simultaneously calculated [1], and the second is the hybrid approach in which the noise source is firstly obtained by solving the unsteady flow and then the related aeroacoustic theories, such as acoustic analogy and theory of vortex sound, are employed to predict the far-field noise. In Engineering, the hybrid approach is more widely employed because it could predict the far-field noise with lower computational cost than the DNS.

The Mach number, Reynolds number and Strouhal number are three important non-dimensional parameters of the cylinder flow. Various researches have shown that the Strouhal number of vortex shedding is usually in the range of 0.22-0.30 for the high Reynolds number ($Re > 1000$) and low Mach number ($Ma < 0.3$) flow. If we define that k and D are the wave number at vortex shedding frequency and the diameter of the cylinder respectively, the non-dimensional wave number $kD = 2\pi \cdot St \cdot Ma$ will be less than 0.5. In this situation, the circular cylinder usually could be regarded as an acoustically compact structure for the prediction of the noise at the vortex shedding frequency, and the diffraction effect of cylinder surface to aerodynamic noise is equivalent to a compact dipole source [2]. Many researchers have validated that the Curle's equation has the ability to predict the cylinder noise at the vortex shedding frequency no matter whether the noise source is obtained by solving the incompressible flow [3] or by solving the compressible flow [4].

But the compactness condition is not valid for the prediction of the high frequency noise, and in this situation, the input data for acoustic analogy must be compressible, even for very low Mach number flow. Otherwise, the Curle's equation or FW-H equation using the free-space Green's function is unable to correctly predict the aerodynamic noise scattered by non-compact surface [4]. Takashi et al [5] has shown that a serious error will exist between the Curle's result and the experimental data for the high frequency noise when the flow is solved using incompressible LES, and the similar result has also been numerically validated by Schram [6]. Howe [7] pointed out that the error is mainly induced by the lack of acoustic fluctuation component on the non-compact surface when the source information is obtained by solving the incompressible Navier-Stokes equation. In order to predict the hydrodynamic noise reflected and scattered by the non-compact circular surface when the noise source is obtained from the incompressible

flow, Takaishi et al [5] and Hu et al [8] have independently developed a boundary element method to compute the tailored Green's function for the non-compact surface, and based on this, the theory of vortex sound and acoustic analogy could be implemented to predict the noise scattered by the circular cylinder. In their contributions, as the tailored Green's function satisfies the non-compact wall boundary conditions, the far field acoustic pressure can be directly expressed as a single volume integral over the sound generating region.

In this study, aerodynamic noise scattered by the circular cylinder is studied by using an integral equation method, which has recently been developed to predict the hydrodynamic noise scattered by the non-compact surface [9]. In this method, Green's function in free space is used, and moreover, the time-consuming volume integral could be ignored and only a surface integral must be numerically calculated. The present paper describes the application of this method to predict the aerodynamic noise of the cylinder flow. The study focuses on the scattering effect of cylinder surface to the propagation of noise at different frequencies.

NUMERICAL TECHNIQUE

Flow Simulation

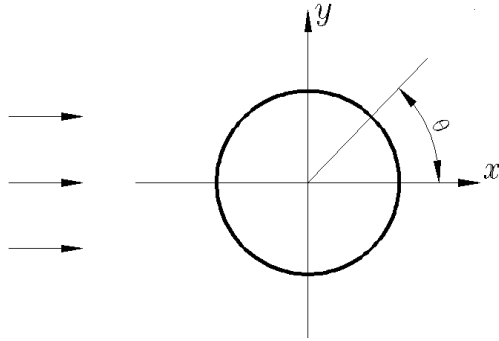


Fig. 1 Schematic of flow over the circular cylinder

As show in Fig. 1, a two dimensional flow over the circular cylinder is simulated by solving the incompressible unsteady Reynolds Averaged Navier-Stokes (URANS) equation. The cylinder diameter D is 0.05m, and the working medium is air with a density of $\rho=1.225\text{kg/m}^3$, and a dynamic viscosity of $\mu=1.7894 \times 10^{-5}\text{kg/m}\cdot\text{s}$. The velocity of the uniform flow in the x direction is $v=34\text{m/s}$, corresponding to the Mach number of $\text{Ma}=0.10$ and the Reynolds number of $\text{Re}=1.16 \times 10^5$. An URANS equation with the Reynolds stress turbulent model has been solved using the Fluent to compute the incompressible viscous flow over the circular cylinder. The computational domain extends from $-10D$ to $20D$ in the streamwise direction and from $-10D$ to $20D$ in the vertical direction. The two-layer method is used to compute the boundary layer flow near the cylinder wall, which requires that the order of $Y^+ \approx 1$ must be employed to ensure adequate resolution. As shown in Fig. 2, the whole computational domain is discretized into multi-domain meshes with 55,000 quadrilateral elements. There are

200 mesh nodes with equal spacing on the wall of the circular cylinder, and the length of each element is $7.85 \times 10^{-4}\text{m}$.

The pressure-velocity coupling is calculated through SIMPLE algorithm. A second order, implicit differencing scheme is used for temporal term, and the second order, upwind and central differencing schemes are used for convection and diffusion terms, respectively. Time step length of the unsteady flow calculation is $\Delta t=10^{-4}\text{s}$. And the convergence criterion of the computation at each time step is that the ratio between the sum of the residuals and the sum of the fluxes for a given variable in all cells should be reduced to 10^{-5} .

A common rule in the solution of acoustic problems is that the element length should be less than 1/10th of the minimum wavelength. The sound speed in air is assumed to be 340m/s, so the top high frequency of the calculated sound is about 40 kHz. Another recommendation, i.e. the time step length of the unsteady flow calculation is 10^{-4}s , and the top frequency of the pressure fluctuation is 5 kHz according to the Nyquist-Shannon sampling theorem. Based on the analysis above, the present study could provide sufficient accuracy up to 5 kHz at best.

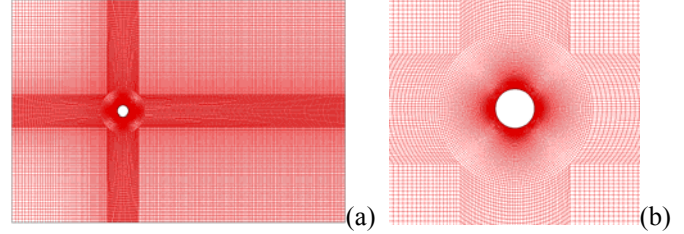


Fig. 2 Computational meshes:(a)whole domain; (b)in the vicinity of cylinder surface

Noise prediction

In our recent work, an integral equation which extended the acoustic analogy was proposed to predict the hydrodynamic noise scattered by the non-compact surface. The detailed derivation process was introduced in reference [9]. And the integral equation is

$$\begin{aligned}
 C(f)p_a(\mathbf{x},t) = & \int_{-T}^T \int_{\Omega} \frac{\partial^2 g}{\partial y_i \partial y_j} T'_{ij} d\mathbf{y} d\tau \\
 & - \int_{-T}^T \int_S \frac{\partial g}{\partial \mathbf{n}(\mathbf{y})} p_h dS(\mathbf{y}) d\tau \\
 & + \int_{-T}^T \int_S \rho_0 v_n^s \frac{\partial g}{\partial \tau} dS(\mathbf{y}) d\tau \\
 & - \int_{-T}^T \int_S \frac{\partial g}{\partial \mathbf{n}(\mathbf{y})} p_a dS(\mathbf{y}) d\tau
 \end{aligned} \tag{1}$$

where \mathbf{x} and \mathbf{y} are the position of observer and source, t and τ are the time of observer and source, respectively. Ω is the nonlinear flow domain which is associated with the generation of acoustic energy, S is the solid surface in arbitrary motion defined by $f = 0$: f is such that $f > 0$ inside the

volume Ω and $f < 0$ outside, g is the time-domain Green's function in free space, v_n^S is the normal velocity of the moving surfaces, p_h is exactly the hydrodynamic force per unit area exerted on the fluid by solid surfaces, p_a is the acoustic pressure, and T'_{ij} is the approximate Lighthill's stress tensor for incompressible flow defined by.

$$T'_{ij} = \rho_0 v_{hi} v_{hj} + (p_0 + p_h - c^2 \rho_0) \delta_{ij} + e_{ij} \quad (2)$$

$C(f)$ is the solid angle, and for the smooth closed surfaces, its value is

$$C(f) = \begin{cases} 1 & f > 0 \\ 1/2 & f = 0 \\ 0 & f < 0 \end{cases} \quad (3)$$

For the low Mach numbers flow around the stationary circular cylinder, the monopole term disappears, and moreover, the noise level radiated from the quadrupole term could be ignored, as its acoustic power is usually much less than that scattering from the solid boundary with finite volume. And implementing the Fourier transform, we could obtain the frequency-domain expression of equation (1) as follows

$$\begin{aligned} C(f)P_a(\mathbf{x}, \omega) + \int_S \frac{\partial G}{\partial \mathbf{n}} P_a(\mathbf{y}, \omega) dS(\mathbf{y}) \\ = - \int_S \frac{\partial G}{\partial \mathbf{n}} P_h(\mathbf{y}, \omega) dS(\mathbf{y}) \end{aligned} \quad (4)$$

where P_a and P_h are the fluctuations of acoustic pressure and hydrodynamic pressure in the frequency domain, respectively. G is the frequency-domain Green's function in free space, and in a two-dimensional space, the expressions of it and its normal derivative are

$$G = \frac{jH_0^{(1)}(k|\mathbf{x} - \mathbf{y}|)}{4} \quad (5)$$

and

$$\frac{\partial G}{\partial \mathbf{n}(\mathbf{y})} = \frac{jk(\mathbf{x} - \mathbf{y}) \cdot \mathbf{n}(\mathbf{y})}{4} H_1^{(1)}(k|\mathbf{x} - \mathbf{y}|) \quad (6)$$

Equation (4) could be solved using the boundary element method.

VALIDATION

To ensure that the numerical method used in the current work produces accurate results, a thorough validation of the computation of both the flow and noise was conducted. The detailed work is introduced as follows.

Flow computation

Distributions of Y^+ around the wall at two different time are plotted in Fig. 3, which meet the requirement of length scale of elements near the wall for two-layer model. And $t=1777\Delta t$ and $t=1803\Delta t$ are respectively the time that the lift coefficient

around the cylinder achieves the positive and negative peak value, where the time development of the pressure fluctuation and vortex shedding and their correlation will be discussed later. Fig. 4 shows the profile of the unsteady pressure coefficient C_p on the cylinder wall. The result displays that the static pressure on the cylinder surface in the range from $\theta=-120^\circ$ (240°) to $\theta=120^\circ$ has a strong fluctuation due to the alternating vortex shedding. Static pressure on the upper surface is higher than that on the lower surface when the vortex is shedding from the upper surface, and vice versa. And the numerical result of the pressure coefficient agrees well with the time-averaged experimental result of Batham [21] at the Reynolds number of $Re=1.1 \times 10^5$.

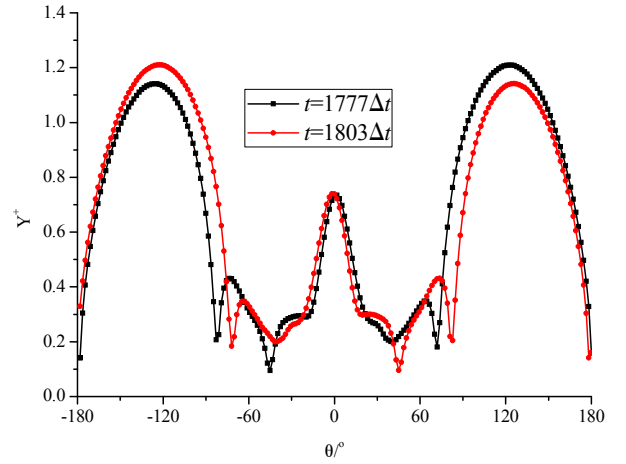


Fig. 3 Distribution of Y^+ on the circular cylinder

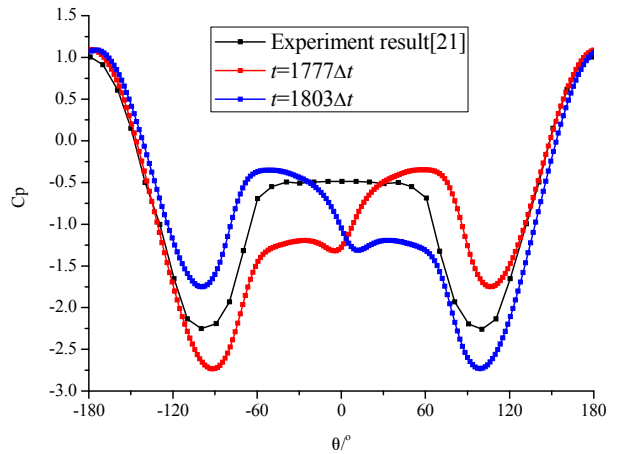


Fig. 4 Comparison of pressure coefficient between numerical result and experimental data

Fig. 5 shows the time histories of lift coefficient C_L and drag coefficient C_D . And the simulation accurately captures the phenomenon that the period of the lift coefficient is twice that of the drag coefficient. And the fundamental frequency of lift

coefficient fluctuation is $f_0 = 192\text{Hz}$, corresponding to the Strouhal number of $St=0.28$.

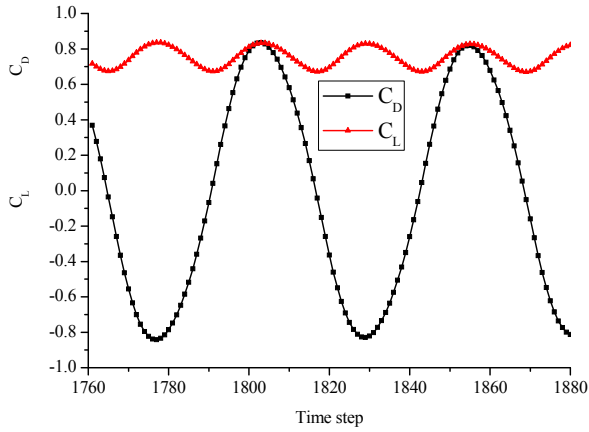


Fig. 5 Time histories of lift and drag coefficient on the circular cylinder

Noise prediction

The code of noise prediction mainly includes the radiation and scattering modules, which are validated as follows. As shown in Fig. 6, the radius of circular cylinder is $a=0.025\text{m}$, and the origin of the Cartesian coordinates system locates at the center of the circular cylinder. The polar coordinates of the point source \mathbf{y} and observer \mathbf{x} are (r_y, θ_y) and (r_x, θ_x) , respectively. Sound pressure radiated from a unit dipole source in the free space is

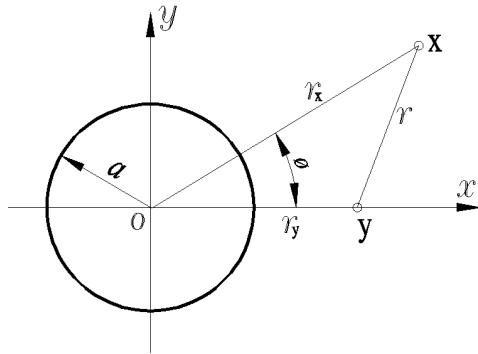


Fig. 6 Schematic of point source scattered by the circular cylinder

$$P_{ID} = \frac{jk}{4} \frac{H_1^{(1)}(kr)}{r} (\mathbf{x} - \mathbf{y}) \cdot \mathbf{n}(\mathbf{y}) \quad (7)$$

And the analytical expression for sound pressure scattered by the circular cylinder is

$$P_{SD} = \frac{j}{4} \sum_{m=0}^{\infty} \varepsilon_m H_m^{(1)}(kr_x) \begin{bmatrix} -m \sin(m\phi) \frac{\partial \theta_y}{\partial \mathbf{n}(\mathbf{y})} A_{ms} \\ +k \cos(m\phi) \frac{\partial r_y}{\partial \mathbf{n}(\mathbf{y})} B_{ms} \end{bmatrix} \quad (8)$$

where $\varepsilon_m = 1$ for $m=0$ and $\varepsilon_m = 2$ for $m>0$, $\mathbf{n}(\mathbf{y})$ is the polar direction of the dipole source, and

$$\phi = \theta_x - \theta_y \quad (9)$$

$$A_m^S = -\alpha_m H_m^{(1)}(kr_y) \quad (10)$$

$$B_m^S = -\alpha_m \left[-H_{m+1}^{(1)}(kr_y) + \frac{m}{kr_y} H_m^{(1)}(kr_y) \right] \quad (11)$$

$$\alpha_m = \frac{J'_m(ka)}{H_m^{(1)}(ka)} = \frac{kaJ_{m+1}(ka) - mJ_m(ka)}{kaH_{m+1}^{(1)}(ka) - mH_m^{(1)}(ka)} \quad (12)$$

In real computation, we define that the dipole source locates at $\mathbf{y} = (0.05, 0)$, the polar direction is $\mathbf{n}(\mathbf{y}) = (1, 0)$ and the wavenumber is $k=40$. The observer locates on the circle with a radius of $r_x=3\text{m}$. The cylinder surface is discretized into 200 uniform elements, and the isoparametric boundary element method is adopted to predict the noise radiated from the dipole source and scattered by the circular cylinder. If we compute the sound pressure when the observer locates at different angular coordinates, we could obtain the directivity pattern of noise radiation. As shown in Fig. 7, good agreement between the numerical result and analytical solution validates the code of noise prediction.

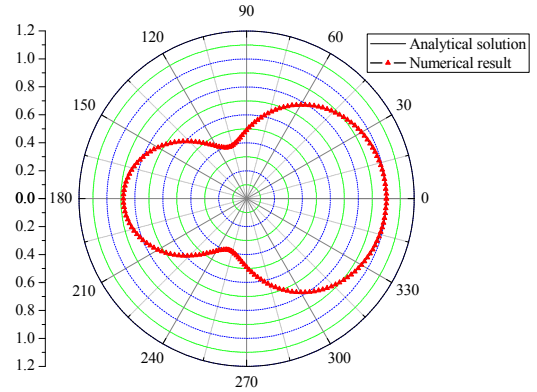


Fig. 7 Directivity pattern of diopole source scattered by the circular cylinder

RESULTS AND DISCUSSIONS

Flow field

Fig. 5 shows that the fluctuation amplitude of lift coefficient is much larger than that of drag coefficient, implying that the noise level associated with the lift force at vortex shedding frequency is much larger than that associated with the drag force, that is to say, the direction of the maximum noise level

will be vertical. As mentioned before, Fig. 5 also shows that the value of the lift coefficient reaches a negative peak at $t=1777\Delta t$ and a positive peak at $t=1803\Delta t$. The instantaneous vorticity fields at $t=1777\Delta t$ and $t=1803\Delta t$ are plotted in Fig. 8(a) and Fig. 8(b), showing the alternating vortex shedding from the lower and upper edge of the cylinder, respectively.

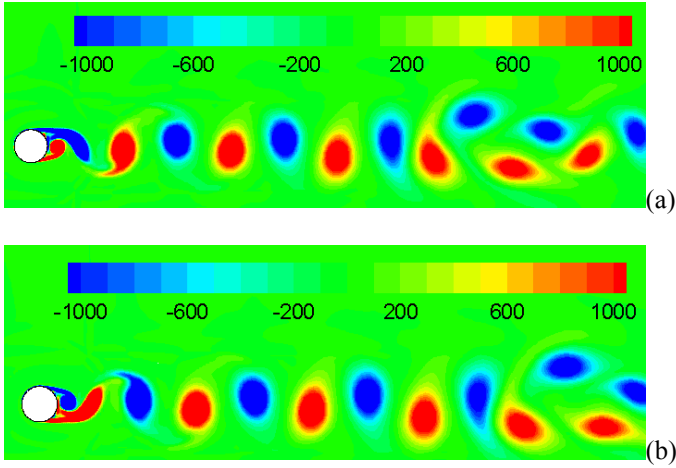


Fig. 8 Time development of the vorticity field: (a) $t=1777\Delta t$; (b) $t=1803\Delta t$

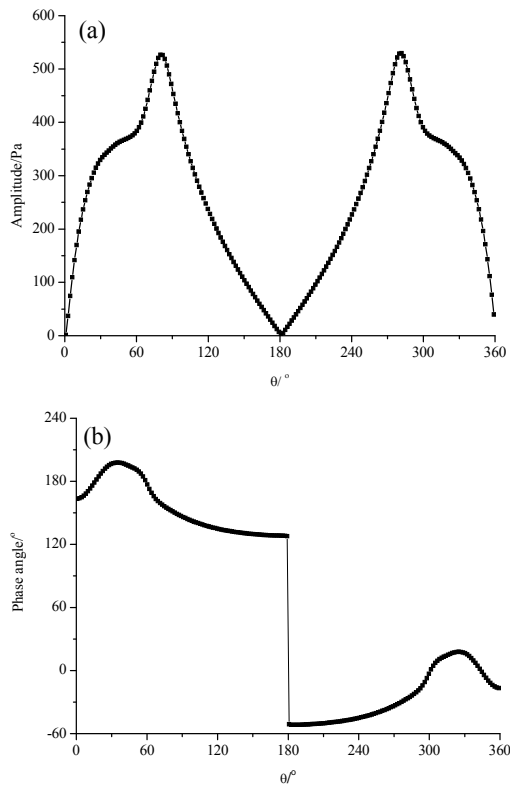


Fig. 9 Pressure fluctuation on the cylinder at the vortex shedding: (a) amplitude; (b) phase angle

Fig. 9 presents the amplitude and phase angle of the pressure fluctuation component at the vortex shedding frequency f_0 . The distribution of pressure fluctuation indicates that its peak values locate exactly on the position of vortex shedding of $\theta=70^\circ$ on the upper surface and $\theta=290^\circ$ on the lower surface of the circular cylinder. Moreover, the phase of pressure fluctuation on the upper surface is just opposite to that on the lower surface.

Acoustic field

As shown in Fig. 1, the sound pressure level at the observer is calculated using the following formulation

$$\text{SPL} = 20 \log_{10} (P_a / P_{\text{ref}}) \quad (13)$$

where $P_{\text{ref}} = 2.0 \times 10^{-5} \text{Pa}$ is the reference pressure.

Fig. 10 shows the directivity pattern of the noise at the low frequencies f_0 and $2f_0$. When the acoustic frequency is f_0 , the direction of the maximum noise level is vertical, which confirms that the noise is mainly induced by the fluctuation of lift force on the cylinder surface. This result is consistent with various numerical results, such as those of Inoue et al [1] using direct numerical simulation, Gloerfelt et al [3] using the Curle's equation, Takaishi et al [5] adopting using vortex sound theory and Hu et al [8] employing the tailored Green's function for circular cylinder. When the acoustic frequency is $2f_0$, the direction of the maximum noise level is horizontal, which also has a good agreement the result of Hu et al [8].

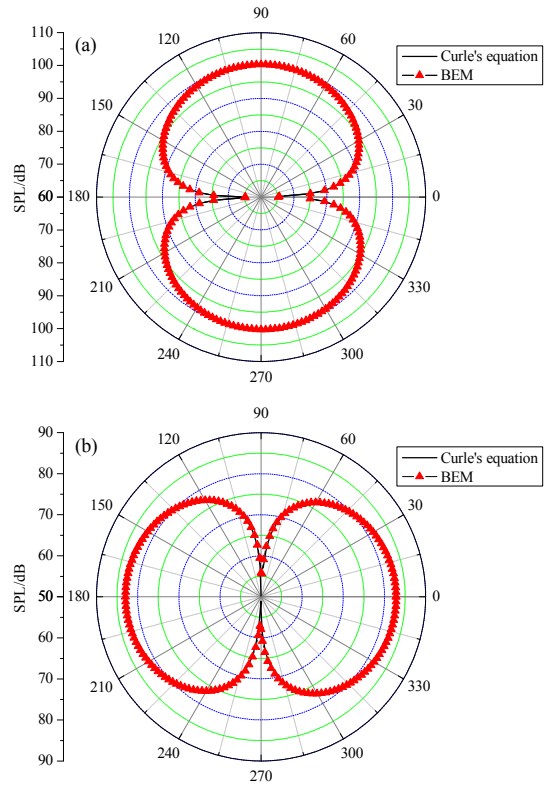


Fig. 10 Directivity pattern of low frequency noise: (a) $f = f_0$; (b) $f = 2f_0$

Moreover, when the acoustic frequencies are f_0 and $2f_0$, the circular cylinder could be regarded as an acoustically compact surface, because the wave lengths, which are 1.770m ($f=f_0$) and 0.885m ($f=2f_0$) respectively, are much larger than the diameter of the cylinder. In this situation, the scattering effect of cylinder to quadrupole noise is equivalent to that on the compact dipole source, so the numerical result of present method has a good agreement with that of the Curle's equation. And Fig. 11 and Fig. 12 plot the noise fields for the two low frequencies in the range of $-1\text{m}\leq x\leq 1\text{m}$ and $-1\text{m}\leq y\leq 1\text{m}$.

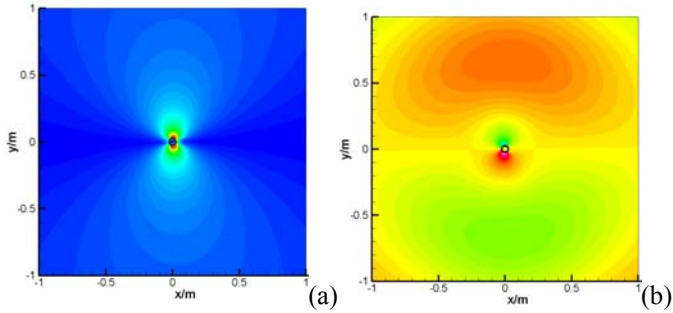


Fig. 11 Distribution of acoustic field for $f=f_0$: (a) absolute value; (b) real part

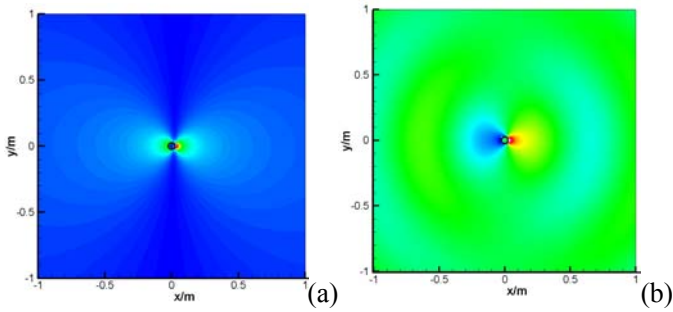


Fig. 12 Distribution of acoustic field for $f=2f_0$: (a) absolute value; (b) real part

For the high frequency noise, the wave lengths are 0.089m ($f=20f_0$) and 0.071m ($f=25f_0$), and the circular cylinder is acoustically non-compact. Numerical result obtained from the Curle's equation has an obvious discrepancy with that obtained from the present method. Fig. 13 compares the directivity patterns of the two results. The one from Curle's equation still gives the typical compact dipole noise feature, which implies that this method could not accurately predict the scattering effect of the non-compact cylinder surface to high frequency noise propagation. But the present result displays a more complicated trefoil-like pattern, which is similar to the numerical result of Takaishi. Moreover, Fig. 14 and Fig. 15 plot the noise fields for the two high frequencies.

Based on the analysis above, the present method has the ability to predict the hydrodynamic noise scattered by the circular cylinder for different frequencies. And compared with

the previous methods, the advantage of the present method is to avoid the time-consuming volume integral.

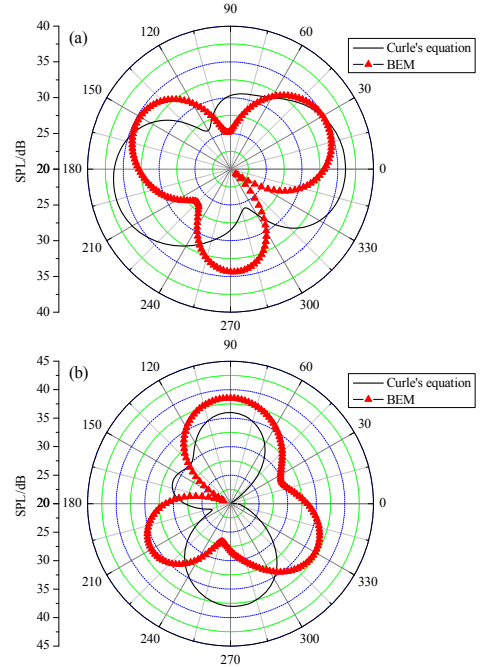


Fig. 13 Directivity pattern of high-frequency noise: (a) $f=20f_0$; (b) $f=25f_0$

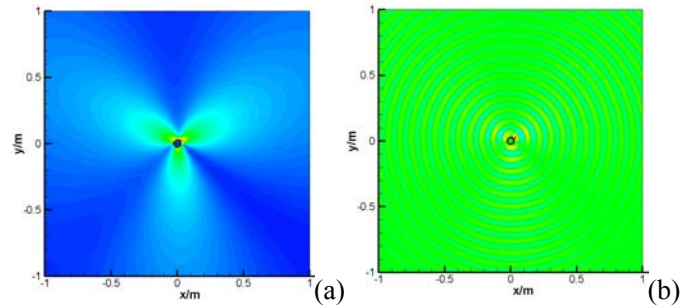


Fig. 14 Distribution of acoustic field for $f=20f_0$: (a) absolute value; (b) real part

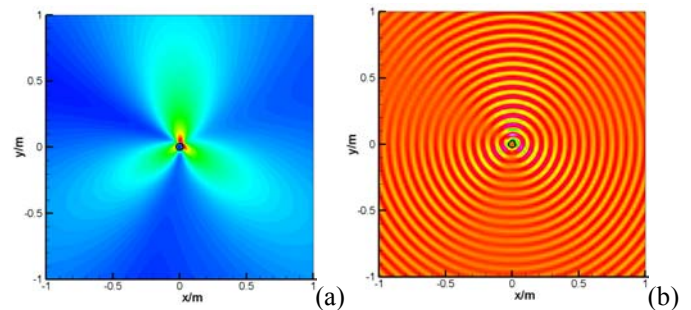


Fig. 15 Distribution of acoustic field for $f=25f_0$: (a) absolute value; (b) real part

CONCLUSIONS

The boundary element method has been applied to compute the noise generated from hydrodynamic flow over a circular cylinder. Numerical results show that the predicted sound pressure level at low frequency using the present method is in good agreement with that using the Curle's equation. However, directivity patterns are quite different at high frequency, where the Curle's equation still gives the feature of compact dipole sound, but the present method gives a more complicated trefoil-like pattern. Further experimental study is expected to validate the numerical result.

ACKNOWLEDGEMENT

This work is funded by the National Natural Science Foundation of China (No.50976084) and Shenyang Blower Works Group Co., Ltd.

REFERENCES

- [1] Inoue O., and Hatakeyama N. Sound generation by a two-dimensional circular cylinder in a uniform flow. *Journal of Fluid Mechanics*, 2002, 471, pp.285-314.
- [2] Curle N. The influence of solid boundaries on aerodynamic sound. *Proceedings of the Royal Society of London, Series A, Mathematics and Physical Sciences*, 1955, 231, pp.505-514
- [3] Gloerfelt X, Perot F, Bailly C, Juve D. Flow-induced cylinder noise formulated as a diffraction problem for low Mach numbers. *Journal of Sound and Vibration*, 2005, 287, pp. 129-151.
- [4] Singer B A, Brentner K S, Lockard D P. Simulation of acoustic scattering from a trailing edge. *Journal of Sound and Vibration*, 2000, 230(3), pp. 541-560.
- [5] Takaishi T, Miyazawa M, Kato C. Computational method of evaluating noncompact sound based on vortex sound theory. *The Journal of Acoustical Society of America*, 2007, 121, pp. 1353-1361.
- [6] Schram C, Anthoine, Hirschberg A. Calculation of sound scattering using Curle's analogy for non-compact bodies. *AIAA Paper 2005-2836*, 2005.
- [7] Howe M S. Edge-source acoustic Green's function for an airfoil of arbitrary chord, with application to trailing-edge noise. *The Quarterly Journal of Mechanics and Applied Mathematics*, 2001, 54, pp.139-155.
- [8] Hu F Q., Guo Y P, and Jones A D. On the computation and application of exact Green's function in acoustic analogy. In *11th AIAA/CEAS Aeroacoustics Conference*, Monterey, California, May 2005, on CD-

ROM.

- [9] Mao Y J, Qi D T, Gu Y Y. Prediction of the low Mach flow induced noise scattered by the non-compact bodies. *Journal of Engineering Thermophysics. Under Review*